

A two-grating method for combined beam splitting and frequency shifting in a two-component laser-Doppler velocimeter

Ari Glezer and Donald Coles

California Institute of Technology, Pasadena, California 91125

(Received 22 June 1982; accepted 24 August 1982)

The use of a rotating radial phase grating to carry out beam splitting and frequency shifting in a laser-Doppler velocimeter is briefly reviewed. This technique is not new. However, the present design adds a substantial new element by using two overlapping radial gratings to produce a two-channel system in which channel separation can be accomplished by electronic filtering of the signal from a single detector.

I. GENERAL DESCRIPTION OF THE OPTICAL ARRANGEMENT

A two-channel dual-scatter laser-Doppler velocimeter (LDV) has been fabricated using the optical arrangement sketched in Fig. 1. The helium-neon laser (Spectra Physics model 124) has a power output of 15 mW. A lens (FL = 45.0 cm) on the laser focuses the output beam in the common plane of two partially overlapping radial phase gratings at a point where the grating lines cross at right angles. The term "common plane" is an approximation; the two grating planes are separated by a gap of a small fraction of a millimeter to provide clearance for rotation. The grating line density at this point is nominally 42 lines/mm. The gratings produce a regular square pattern of diverging diffracted beams, with much of the energy concentrated in the four first-order beams. Two of these four beams lie in a vertical plane, and two lie in a horizontal plane.

The four first-order beams are at once isolated by a mask. They are made parallel by a fixed primary lens (FL = 66.0 cm) which is mounted with its focal point in the grating plane. A movable secondary lens (FL = 62.9 cm) then causes the four beams to focus and cross at a point which defines the center of the LDV test volume. Depending on circumstances, the velocity component normal to the optical axis can be measured in a plane defined by any two of the four beams. For two-component measurements close to a wall, only three beams are used, as described in Sec. IV.

The receiving optics at present consist of a collecting

lens and a single photodiode (Texas Instruments model TIED 83, with model TIEF 152 amplifier). The photodiode has a small active area (0.25 mm in diameter) and serves as its own pinhole.

II. DESIGN OF THE DIFFRACTION GRATINGS

A diffraction grating imposes on an incident light wave a spatially periodic variation of amplitude or phase or both. An adequate analysis can be based on an approximation called Fraunhofer diffraction, which applies when both the light source and the observation point are far from the grating.

For a plane grating normal to the optical or z axis, the electromagnetic field $\mathbf{E}(\mathbf{r})$ at a specified observation point is described by the expression¹

$$\mathbf{E}(\mathbf{r}) = \frac{i}{\lambda} \mathbf{E}(0) \frac{e^{-2\pi i R/\lambda}}{R} \hat{t}(u, v), \quad (1)$$

where $\mathbf{E}(0)$ is the (uniform) field incident on the grating, λ is the wave length of the incident light, R is the distance from the grating to the point of observation, and

$$\hat{t}(u, v) = \iint_{-\infty}^{\infty} t(x', y') e^{-2\pi i (ux' + vy')} dx' dy' \quad (2)$$

is the two-dimensional Fourier transform of the transmission function $t(x', y')$ which relates the transmitted field \mathbf{E}_t at the grating to the incident field \mathbf{E}_i ; i.e., $\mathbf{E}_t(\mathbf{r}') = t(\mathbf{r}')\mathbf{E}_i(\mathbf{r}')$. The transformed variables u and v are defined as $u = \alpha/\lambda$ and $v = \beta/\lambda$, where α and β are the direction cosines of the observation point with respect to the origin.

Let a one-dimensional phase grating be defined by $\beta = v = 0$, by an amplitude transmission function of unity, and by a phase transmission function $t(x') = e^{i\psi(x')}$, where ψ is a periodic function of x' with period d , say. In this case the transform

$$\hat{t}(u, 0) = \delta(\beta) \sum_{m=-\infty}^{\infty} \frac{1}{d} \delta\left(u - \frac{m}{d}\right) \times \int_{-d/2}^{d/2} t(x') e^{-2\pi i u x'} dx' \quad (3)$$

contains only discrete peaks in directions $u = m/d$ in the plane $\beta = 0$, as indicated by the delta functions. The diffracted beams form angles $\theta^{(m)} = \arcsin(\lambda m/d)$ with respect to

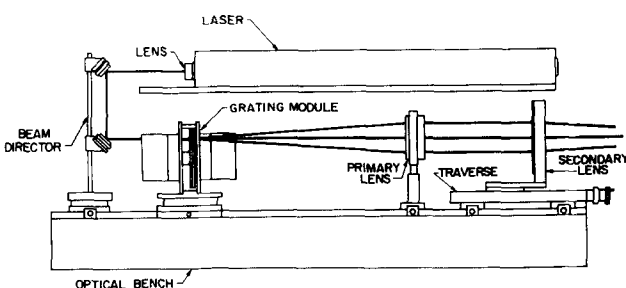


FIG. 1. A side view of the two-channel LDV system. The optical bench is 120 cm long. The heavy lines indicate laser beams. The traverse mechanism at the right moves the LDV test volume along the optical axis. The distance between the grating module and the primary lens is not to scale.

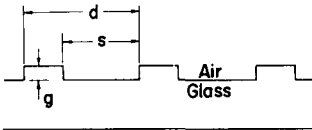


FIG. 2. Cross section of a two-dimensional phase grating.

the incident beam.

In the simplest case, the grating may be taken as a transparent plate with periodically varying thickness $G(x')$. The phase change imposed on the incident light is then $\psi(x') = (2\pi/\lambda)(n-1)G(x')$, where n is the index of refraction.

Suppose that such a phase grating is realized by etching parallel rectangular grooves of width s , depth g , and spacing d in a glass substrate, as shown in Fig. 2. The phase variation is then given by the specific function

$$\begin{cases} \psi = -\frac{1}{2}\pi M, & -\frac{1}{2}s < x' < \frac{1}{2}s, \\ \psi = \frac{1}{2}\pi M, & \frac{1}{2}s < x' < d - \frac{1}{2}s, \end{cases} \quad (4)$$

where $M = 2(n-1)g/\lambda$, and Eq. (3) becomes

$$\hat{i}(u,0) = \delta(\beta) \sum_{m=-\infty}^{\infty} \frac{\delta(u - m/d)}{\pi u d} \times \left(2i \sin \frac{\pi M}{2} \sin \pi u(d-s) + e^{-i\pi M/2} \sin \pi u d \right). \quad (5)$$

From Eqs. (1) and (5), the electromagnetic field for a given direction $u = m/d$ is

$$\begin{aligned} \mathbf{E}^{(m)}(\mathbf{r}) = \frac{i}{\lambda} \mathbf{E}(0) \frac{e^{-2\pi i R/\lambda}}{R} \\ \times \delta(\beta) \left[2i \left(1 - \frac{s}{d} \right) \sin \frac{\pi M}{2} \frac{\sin m(1-s/d)}{\pi m(1-s/d)} \right. \\ \left. + e^{-i\pi M/2} \frac{\sin \pi m}{\pi m} \right]. \end{aligned} \quad (6)$$

In particular, for $m = 0$,

$$\begin{aligned} \mathbf{E}^{(0)}(\mathbf{r}) = \frac{i}{\lambda} \mathbf{E}(0) \frac{e^{-2\pi i R/\lambda}}{R} \delta(\beta) \\ \times \left[2i \left(1 - \frac{s}{d} \right) e^{i\pi M/2} + \frac{s}{d} e^{-i\pi M/2} \right]. \end{aligned} \quad (7)$$

Define the relative intensity (or diffraction efficiency) for the various orders as $\eta^{(m)} = |\mathbf{E}^{(m)}(\mathbf{r})|^2 / |\mathbf{E}(\mathbf{r})|^2$. Then

$$\begin{cases} \eta^{(0)} = 1 - 2 \frac{s}{d} \left(1 - \frac{s}{d} \right) (1 - \cos \pi M), \\ \eta^{(m)} = 4 \left(1 - \frac{s}{d} \right)^2 \sin^2 \frac{\pi M}{2} \left(\frac{\sin \pi m(1-s/d)}{\pi m(1-s/d)} \right)^2. \end{cases} \quad (8)$$

These results are not new. They have previously been obtained in a slightly different form by Sirohi and Blume² and have been discussed by Oldengarm *et al.*³

If the grating is moving (say) with a constant linear velocity U in the x' direction, the diffraction pattern does not change, but the frequency in each of the diffraction directions is increased or decreased by an amount proportional to the sine of the diffraction angle and to the grating velocity. In Eq. (2), change the variable x' to $x'' - Ut$ to obtain, in an obvious notation,

$$\begin{aligned} \mathbf{E}_u^{(m)}(\mathbf{r}) = \frac{i}{\lambda} \mathbf{E}(0) \frac{e^{-2\pi i R/\lambda}}{R} e^{2\pi i u t} \\ \times \int_{-\infty}^{\infty} t(x'', y') e^{-2\pi i (u x'' + v y')} dx'' dy' \\ = \mathbf{E}^{(m)}(\mathbf{r}) e^{2\pi i u t}. \end{aligned} \quad (9)$$

Since $u = m/d$, the frequency shift in each diffracted order is

$$f^{(m)} = uU = (m/d)U. \quad (10)$$

This shift is positive in the direction of motion of the grating.

In this idealized analysis, the grating and the incident light beam have been taken to be one-dimensional and infinite in extent. The actual light source is a focused laser beam having a finite diameter and a Gaussian distribution of intensity. The number of grating lines encountered by the beam is finite, but can be made relatively large. The function $\hat{i}(u, v)$ is then continuous, but still very strongly peaked near $u = m/d$.

The fact that the grating lines are not parallel in a radial grating is not a serious defect. If the disc rotates with angular velocity Ω and the incident beam is at radius $D/2$ from the center of rotation, the frequency shift in the diffracted beam of order m is $f^{(m)} = m\Omega D/2d$, where the line pitch d is related to the total number of lines N by $d = \pi D/N$. Consequently,

$$f^{(m)} = mN\Omega/2\pi. \quad (11)$$

The frequency shift in each order thus depends only on the total number of lines on the disc and on the angular velocity of the disc; it does not depend on the radius $D/2$ or on the wavelength of the incident light. The diffracted beams will, however, have a very slightly distorted cross section.

III. FABRICATION OF THE DIFFRACTION GRATINGS

The use of radial diffraction gratings to perform the functions of beam splitting and frequency shifting in an LDV system is not new (e.g., Stevenson).⁴ Neither is the use of bleached or etched phase gratings, rather than amplitude gratings, to increase the relative intensity of the first-order diffracted beams (e.g., Wigley⁵; Oldengarm *et al.*).³ What is new in the present system is the use of two identical overlapping gratings to produce a compact two-component LDV system in which channel separation can be achieved by electronically filtering the signal from a single detector. Also new is the use of digital techniques to remove deterministic noise generated by nonuniform rotation rate and nonuniform line spacing of the gratings. This latter feature is described in an Appendix.

It was our intention in the present system to use gratings designed for maximum efficiency in the first-order diffracted beams [i.e., $s/d = \frac{1}{2}$ and $2(n-1)g/\lambda = 1$, in the notation of Sec. II]. All even orders, including zero order, should be absent, and the energy in each of the first-order beams produced by a single grating should be approximately 40% of the incident energy.

The grating discs were manufactured by Teledyne Gurely, who cooperated with the authors in the development. An existing 16 384 line master was used. The substrate mate-

rial is optical quality glass. The discs are 13.84 cm in diameter and approximately 0.6 cm thick. The discs were ground and polished to be flat and of uniform thickness to within one wavelength per cm. The line pattern etched in the glass forms a track with an inner radius of 5.66 cm and an outer radius of 6.82 cm. The track is concentric with the outside diameter to $25 \mu\text{m}$ or better. To maximize the intensity in the first-order beams, the groove width s was specified to be half the line pitch d , and the depth of etching was calculated for the known index of refraction (C-1 glass; $n = 1.5235$). There was apparently some difficulty in controlling the depth of etching, and several samples had to be made before the result was acceptable. A scanning-electron-microscope photograph⁶ of a cut through one early test sample is shown in Fig. 3. The final product has a value of s/d greater than 0.50 and an etching depth different from the specified dimension. As a result, the energy in each of the first-order beams for a single grating is reduced to approximately 30% of the incident energy, and even-order beams are present in the pattern. In practice, the presence of the zero-order beam turns out to be very useful for aligning the optical system. There is some loss of intensity arising from the fact that the gratings, and most of the optical surfaces in the experimental apparatus described in Sec. V as well, are not antireflection coated. Nevertheless, the available laser power of 15 mW is quite sufficient to provide a satisfactory Doppler signal at the detector.

IV. FREQUENCY SHIFTING

Each of the grating discs is attached to a stainless-steel hub and mounted on the shaft of a hysteresis-synchronous motor (Beau model 40H-36, 40H-96). The motors face each other in a box structure, as shown in Fig. 4, with the discs partially overlapping and the etched tracks also facing each other. Runout and wobble are less than $10 \mu\text{m}$ (0.0005 in.). Each motor has three selectable synchronous speeds (1800–900–450 rpm for one motor; 1200–600–300 rpm for the other) when powered by the 60 Hz line.

If the two gratings rotate independently of each other,

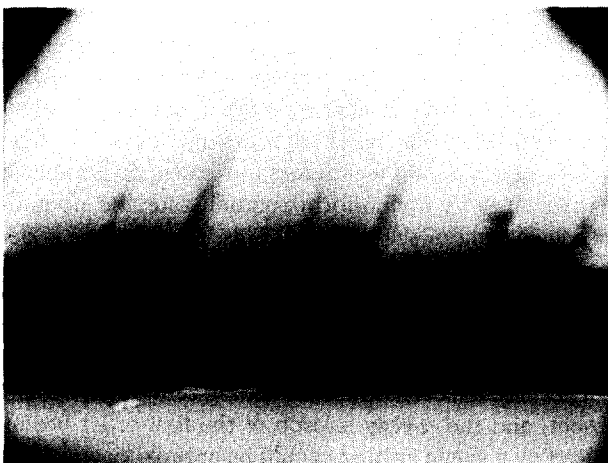


FIG. 3. A scanning-electron-microscope photograph showing a cross section through the etched grating. The magnification is 1400 times. The pitch of the grating is about $24 \mu\text{m}$.

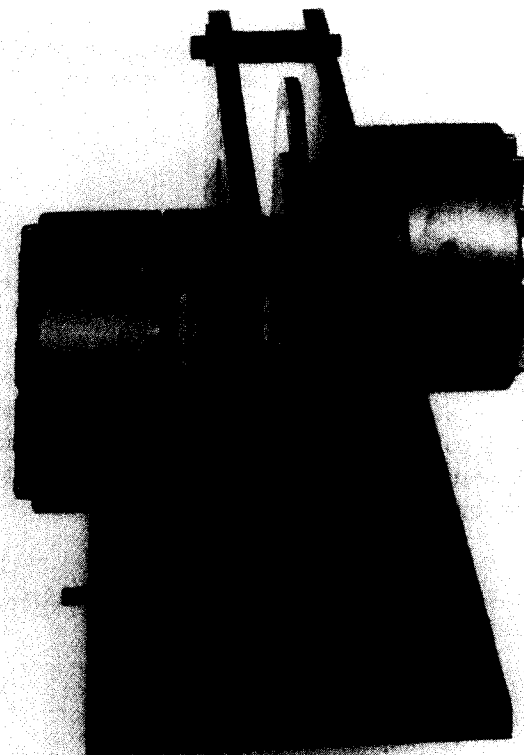


FIG. 4. A photograph showing the grating module. The grating discs are 13.8 cm in diameter. The lateral distance between the two gratings is adjustable.

each of the diffracted beams undergoes two successive frequency shifts; thus,

$$f_1^{(m)} + f_2^{(n)} = (1/2\pi)(mN_1\Omega_1 + nN_2\Omega_2). \quad (12)$$

Various modes of operation suggest themselves. In the mode used for the bulk of the present measurements, as illustrated in Fig. 5, typical bias frequencies (Doppler frequencies for a particle at rest) for the first-order beams in the vertical and horizontal planes are

$$\begin{aligned} F_1 &= |2f_1 - 2f_2|, \\ F_2 &= |2f_1 + 2f_2|. \end{aligned} \quad (13)$$

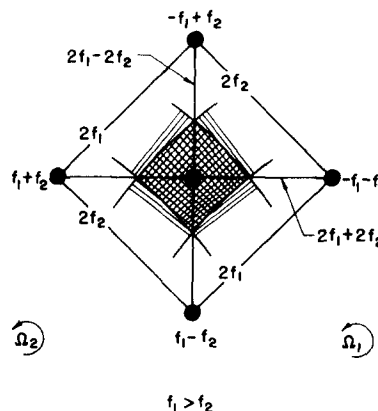


FIG. 5. The beam geometry, showing interactions of the various bias frequencies for the standard two-channel LDV system with both gratings rotating.

In principle and in practice, the separation between F_1 and F_2 can be made sufficiently large so that a single detector can sense the Doppler signal from both channels simultaneously, and the two signals can be subsequently separated electronically by bandpass filtering. The numerical values of f_1 and f_2 can be varied by changing Ω_1 , Ω_2 , and the direction of rotation of the gratings. Note that reversing the direction of rotation of one grating interchanges the two channels. For example, $|2f_1 + 2f_2|$ becomes $|-2f_1 + 2f_2|$ and $|2f_1 - 2f_2|$ becomes $|-2f_1 - 2f_2|$. This property can be valuable if the mean values and/or the dynamic ranges of the two velocity signals are not initially known.

The four-beam geometry also provides velocity information in directions along the perimeter of the pattern in Fig. 5, with bias frequencies $2f_1$ and $2f_2$. This information can be useful for measurements close to a wall, or as a check on system accuracy. Any three of the four beams in Fig. 5 are evidently sufficient to determine two velocity components. In the notation of Fig. 6, let U and V be the velocity components normal and parallel to the wall and let U' be the velocity component along one diagonal at an angle of 45° to the wall. The angle θ between the two beams which are equidistant from the wall differs from the angle θ' between the beams which lie along the chosen diagonal. Let C and C' be the corresponding Doppler constants (in cm/sec per kHz, say) for V and U' , respectively. Evidently,

$$\frac{C}{C'} = \frac{\sin(\theta'/2)}{\sin(\theta/2)} = \frac{1}{\sqrt{2}}. \quad (14)$$

Let $v = V/C$ and $v' = U'/C'$ be the residual Doppler frequencies after subtraction of the bias frequencies. It follows from the sketch that

$$V = Cv, \quad (15)$$

$$U = \sqrt{2}U' - V = \sqrt{2}C'v' - Cv = C(2v' - v).$$

The photodetector signal usually contains either four or three bias frequencies ($2f_1 + 2f_2$, $2f_1 - 2f_2$, $2f_1$, $2f_2$), depending on the beam geometry. The unwanted frequency information is filtered out electronically. This unwanted information can also be eliminated *a priori* from the photodetector signal by using a two-color laser. The four-beam pattern shown in Fig. 5 becomes two concentric four-beam patterns, each corresponding to one of the laser colors. The spatial separation between the concentric patterns is determined by the different diffraction angles for the different wavelengths in the incident beam (see Sec. II). In the standard four-beam

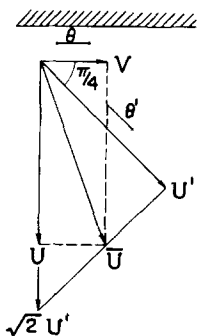


FIG. 6. Velocity measurements close to a wall using a three-beam arrangement.

mode, different laser colors may be chosen for the vertical and horizontal planes, say green and blue, respectively. The undesired color in each plane can be blocked either by a mask, if spatial separation is sufficient, or by a line filter. Velocity information in directions along the perimeter of the pattern corresponding to Fig. 5 is effectively suppressed because of the very high bias frequency for beams of different colors. In the three-beam mode just described, one of the green beams in the vertical plane can be permanently blocked. Once the bias frequency for the blue beams in the horizontal plane is fixed, the bias frequency for the second or green channel can be set to either $2f_1$ or $2f_2$ by unblocking either the left or right green beam in the horizontal plane. A single detector can still be used to sense the Doppler signal from both channels.

V. EXPERIMENTAL APPLICATION

The LDV system described in this paper, together with a two-channel tracking processor, was fabricated especially for a detailed study of a turbulent vortex ring (Glezer).⁷ The ring was formed by a momentary jet discharge from a submerged orifice into a glass tank filled with distilled water. The water, including the jet fluid, was uniformly seeded with latex particles (styrene divinylbenzene 6PIC, manufactured by Dow Diagnostics) having a nominal diameter of $5.7 \mu\text{m}$. Seeding concentration was about 2×10^4 particles/cm³, with an average of approximately 10 particles in the focal volume at any instant.

Two-channel measurements of the velocity field associated with a particular turbulent vortex ring were made for an ensemble of realizations at each of numerous locations in the glass tank. The data obtained were ensemble-averaged and used to verify the expected similarity properties of the turbulent vortex ring and to determine mean particle paths and mean vorticity contours in appropriate nonsteady similarity coordinates. Most previous studies of vortex rings have suffered from effects of probe interference and/or directional ambiguity in the measurements of velocity, whether the instrumentation used was the hot-wire anemometer or the LDV. The use of LDV instrumentation with frequency bias eliminates directional ambiguity (as well as probe interference) from the measurements of velocity. The use of a two-channel system also mitigates a difficulty which is peculiar to the turbulent vortex ring, namely substantial dispersion in both space and time for the trajectories of individual rings. This problem of dispersion is inherent in the dynamics of the phenomenon, and the key to its solution is the simultaneous measurement of two independent velocity components; e.g., components parallel and perpendicular to the nominal axis of symmetry of the vortex ring. The resulting information makes possible a technique of pattern recognition in two dimensions which compensates for dispersion and allows the desired mean-velocity data to be obtained from relatively small ensembles.

ACKNOWLEDGMENTS

The research described in this paper was supported by the National Science Foundation under Grant No. CME-7723541.

APPENDIX: GRATING NOISE AND ITS REMOVAL

In the LDV system described here, noise in the photo-detector signal (both channels) includes a periodic component corresponding to apparent velocity fluctuations of about one cm/sec peak to peak. These fluctuations are present when the fluid is at rest and are synchronized with rotation of the gratings. Two dominant periods are associated with each motor: they are the period per revolution and the period per pole. The most likely causes include slight variations in glass thickness and/or etching depth, slight irregularities in line spacing, and slight variations in motor speed (primarily cogging).

A straightforward method for removing the apparent velocity fluctuations is to synchronize the grating rotation with data sampling. A frequency in the range from 50 to 70 Hz for each motor is derived by division from a 1-kHz crystal-controlled pulse train which serves as a pacer for the computer-controlled data-acquisition system. This frequency is transformed to a sine wave and is fed to one channel of a high-fidelity stereo power amplifier (SAE model 2200) equipped with step-up transformers to provide the voltage required by the motors.

Figure 7 is a typical record of grating noise, showing an initial rms level of about 0.7 cm/sec together with several steps in its removal. The sampling rate was 1 kHz and the duration of the record was one second. The four-pole motor was driven at approximately 1071 rpm (in the eight-pole switch position) by a frequency of 1000/14 Hz. The rotation period was 56 msec and the pole period was 7 msec. The six-pole motor was driven at 1250 rpm by a frequency of 1000/16 Hz. The rotation period was 48 msec and the pole period was 8 msec. These four periods being precisely known, amplitude and phase could be accurately determined for each noise component by Fourier analysis. When all four components are subtracted from the original data, the residual fluctuations in the measured frequency correspond to rms velocity fluctuations of about 0.06 cm/sec, as shown in the lowest trace in Fig. 7. These residual fluctuations may be due in part to mechanical vibration of the structure which supports the transmitting optics.

To take advantage of this technique for noise suppression, data acquisition should include a preliminary data record, with the fluid either stationary or flowing with constant velocity. This preliminary record can be analyzed in the manner just described to find the grating noise signal,

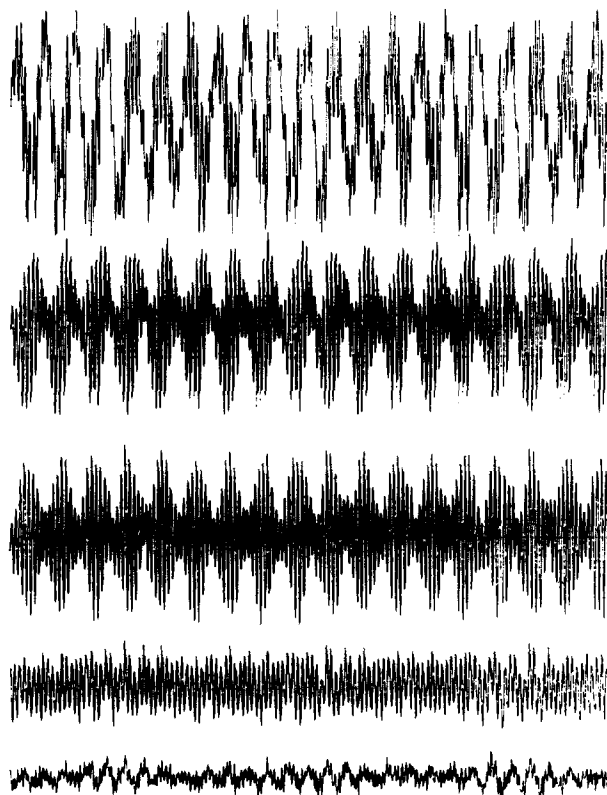


FIG. 7. Grating noise and its removal, as practiced during the vortex-ring experiments. Top trace: original signal. 2nd trace: 48 msec period removed. 3rd trace: 56 msec period also removed. 4th trace: 7 msec period also removed. 5th trace: 8 msec period also removed.

which is then subtracted from all subsequent data records. The relative location of the latter records in time is presumably controlled by the computer and is therefore accurately known.

¹M. V. Klein, *Optics* (Wiley, New York, 1970).

²R. S. Sirohi and H. Blume, *Opt. Acta* **22**, 943 (1975).

³J. Oldengarm, A. H. vanKreiken, and H. J. Raterink, in *Proceedings ISL / AGARA Workshop on Laser Anemometry* (French-German Research Institute, St. Louis, 1976), p. 603.

⁴W. H. Stevenson, *Appl. Opt.* **9**, 649 (1970).

⁵E. Wigley, A.E.R.E. Harwell, Rep. AERE-R-7886 (1974).

⁶This photograph was obtained through the courtesy of Kenneth Evans of the Jet Propulsion Laboratory, Pasadena, California.

⁷A. Glezer, Ph.D thesis, California Institute of Technology, 1981.